REGULAR ARTICLE

blood advances

Hmga2 collaborates with *JAK2*V617F in the development of myeloproliferative neoplasms

Koki Ueda,[1] Kazuhiko Ikeda,[1,2] Takayuki Ikezoe,[1] Kayo Harada-Shirado,[1,2] Kazuei Ogawa,[1] Yuko Hashimoto,[3] Takahiro Sano,[1] Hiroshi Ohkawara,[1] Satoshi Kimura,[1] Akiko Shichishima-Nakamura,[1] Yuichi Nakamura,[4] Yayoi Shikama,[5] Tsutomu Mori,[6] Philip J. Mason,[7] Monica Bessler,[7] Soji Morishita,[8] Norio Komatsu,[8] Kotaro Shide,[9] Kazuya Shimoda,[9] Shuhei Koide,[10] Kazumasa Aoyama,[10] Motohiko Oshima,[10] Atsushi Iwama,[10] and Yasuchika Takeishi[4]

[1]Department of Hematology, [2]Department of Blood Transfusion and Transplantation Immunology, [3]Department of Diagnostic Pathology, [4]Department of Cardiovascular Medicine, and [5]Department of Pharmacology, Fukushima Medical University, Fukushima, Japan; [6]Department of Human Lifesciences, Fukushima Medical University School of Nursing, Fukushima, Japan; [7]Department of Hematology, The Children's Hospital of Philadelphia, Philadelphia, PA; [8]Department of Hematology, Juntendo University School of Medicine, Tokyo, Japan; [9]Department of Gastroenterology and Hematology, Faculty of Medicine, University of Miyazaki, Miyazaki, Japan; and [10]Department of Cellular and Molecular Medicine, Chiba University Graduate School of Medicine, Chiba, Japan

Key Points

- In patients with MPNs, repression of *MIRlet-7* and mutations in the polycomb genes *EZH2* and *ASXL1* correlate with *HMGA2* overexpression.
- *Hmga2* overexpression collaborates with *JAK2*V617F to promote lethal MPN in mice, highlighting the crucial role of Hmga2.

High-mobility group AT-hook 2 (*HMGA2*) is crucial for the self-renewal of fetal hematopoietic stem cells (HSCs) but is downregulated in adult HSCs via repression by *MIRlet-7* and the polycomb-recessive complex 2 (PRC2) including EZH2. The *HMGA2* messenger RNA (mRNA) level is often elevated in patients with myelofibrosis that exhibits an advanced myeloproliferative neoplasm (MPN) subtype, and deletion of *Ezh2* promotes the progression of severe myelofibrosis in *JAK2*^{V617F} mice with upregulation of several oncogenes such as *Hmga2*. However, the direct role of *HMGA2* in the pathogenesis of MPNs remains unknown. To clarify the impact of *HMGA2* on MPNs carrying the driver mutation, we generated Δ*Hmga2*/*JAK2*^{V617F} mice overexpressing Hmga2 due to deletion of the 3′ untranslated region. Compared with *JAK2*^{V617F} mice, Δ*Hmga2*/*JAK2*^{V617F} mice exhibited more severe leukocytosis, anemia and splenomegaly, and shortened survival, whereas severity of myelofibrosis was comparable. Δ*Hmga2*/*JAK2*^{V617F} cells showed a greater repopulating ability that reproduced the severe MPN compared with *JAK2*^{V617F} cells in serial bone marrow transplants, indicating that Hmga2 promotes MPN progression at the HSC level. Hmga2 also enhanced apoptosis of *JAK2*^{V617F} erythroblasts that may worsen anemia. Relative to *JAK2*^{V617F} hematopoietic stem and progenitor cells (HSPCs), over 30% of genes upregulated in Δ*Hmga2*/*JAK2*^{V617F} HSPCs overlapped with those derepressed by *Ezh2* loss in *JAK2*^{V617F}/*Ezh2*$^{Δ/Δ}$ HSPCs, suggesting that Hmga2 may facilitate upregulation of Ezh2 targets. Correspondingly, deletion of *Hmga2* ameliorated anemia and splenomegaly in *JAK2*^{V617F}/*Ezh2*$^{Δ/wild\text{-}type}$ mice, and *MIRlet-7* suppression and PRC2 mutations correlated with the elevated *HMGA2* mRNA levels in patients with MPNs, especially myelofibrosis. These findings suggest the crucial role of HMGA2 in MPN progression.

Introduction

Myeloproliferative neoplasms (MPNs), including polycythemia vera (PV), essential thrombocythemia (ET), and primary myelofibrosis (primary MF [PMF]), are characterized by the chronic proliferation of mature myeloid cells, extramedullary hematopoiesis, and progression to MF or acute leukemia.[1-3] Mutations in

Submitted 7 January 2017; accepted 18 May 2017. DOI 10.1182/bloodadvances.2017004457.

The data reported in this article have been deposited in the Gene Expression Omnibus database (accession number GSE87464).

The full-text version of this article contains a data supplement.

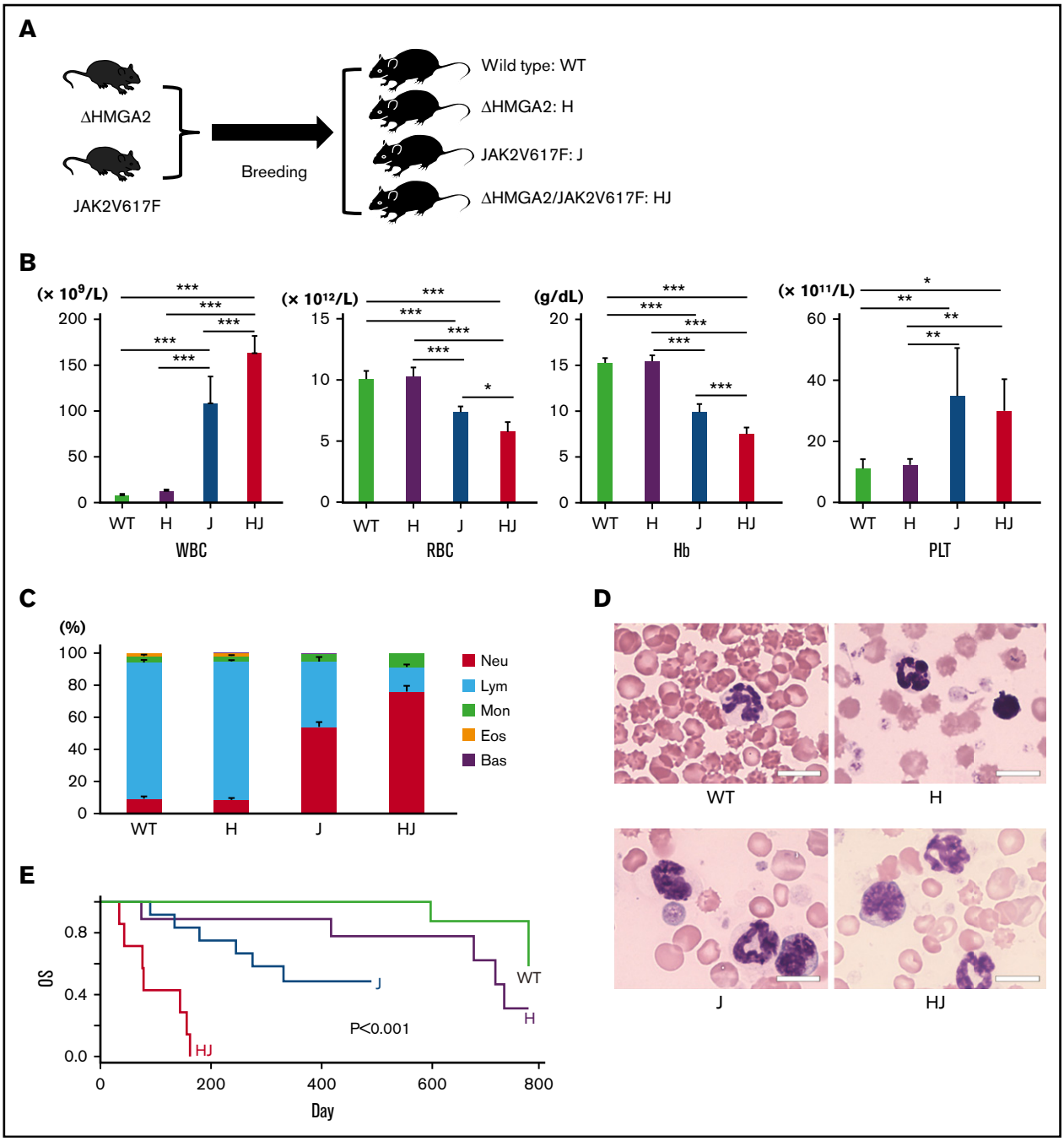

Figure 1. Progressive MPN in Δ*Hmga2/JAK2*^{V617F} mice. (A) Schematic diagram of the experiment. WT, Δ*Hmga2* (H), *JAK2*^{V617F} (J), and Δ*Hmga2/JAK2*^{V617F} (HJ) mice were obtained in predicted Mendelian ratios. The analyses were performed at 12 weeks old. (B) Complete blood cell counts (means ± standard error of the mean [SEM]) and (C) fractions of white blood cells (%) in 5 WT, 7 H, 5 J, and 4 HJ mice. **P* < .05; ***P* < .01; ****P* < .001 calculated by the Tukey-HSD test. (D) May-Giemsa stains of peripheral blood samples (original magnification ×1000). Scale bars indicate 50 μm. (E) Survival periods. N = 9 for WT, 9 H, 12 J, and 7 HJ mice. The *P* values were calculated by a log-rank test. Bas, basophil; Eos, eosinophil; Hb, hemoglobin concentration (g/dL); Lym, lymphocyte; Mon, monocyte; Neu, neutrophil; OS, overall survival; PLT, platelet count (×10^{11}/L); RBC, red blood cell count (×10^{12}/L); WBC, white blood cell count (×10^{9}/L).

JAK2,[4,5] *CALR*,[6,7] and *MPL*[8] are established drivers of myeloproliferation. Expression of *JAK2*V617F in mice can reproduce PV, ET, or MF phenotype,[9-14] but the role of driver mutations in clonal expansion and disease progression has not been well defined. Mutations in epigenetic modifiers, such as *TET2*,[15] *DNMT3A*,[16,17] *ASXL1*,[18] and *EZH2*,[19] and the aberrant expression of microRNAs[20] might lead to MPN progression by altering gene expression, but their targets are largely unknown.

We[21] and others[22] recently demonstrated elevation of the proto-oncogene, high-mobility group AT-hook 2 (*HMGA2*) messenger RNA (mRNA) in granulocytes and CD34^{+} cells of patients with MPNs, especially in PMF with the worst outcome among MPNs.[23]

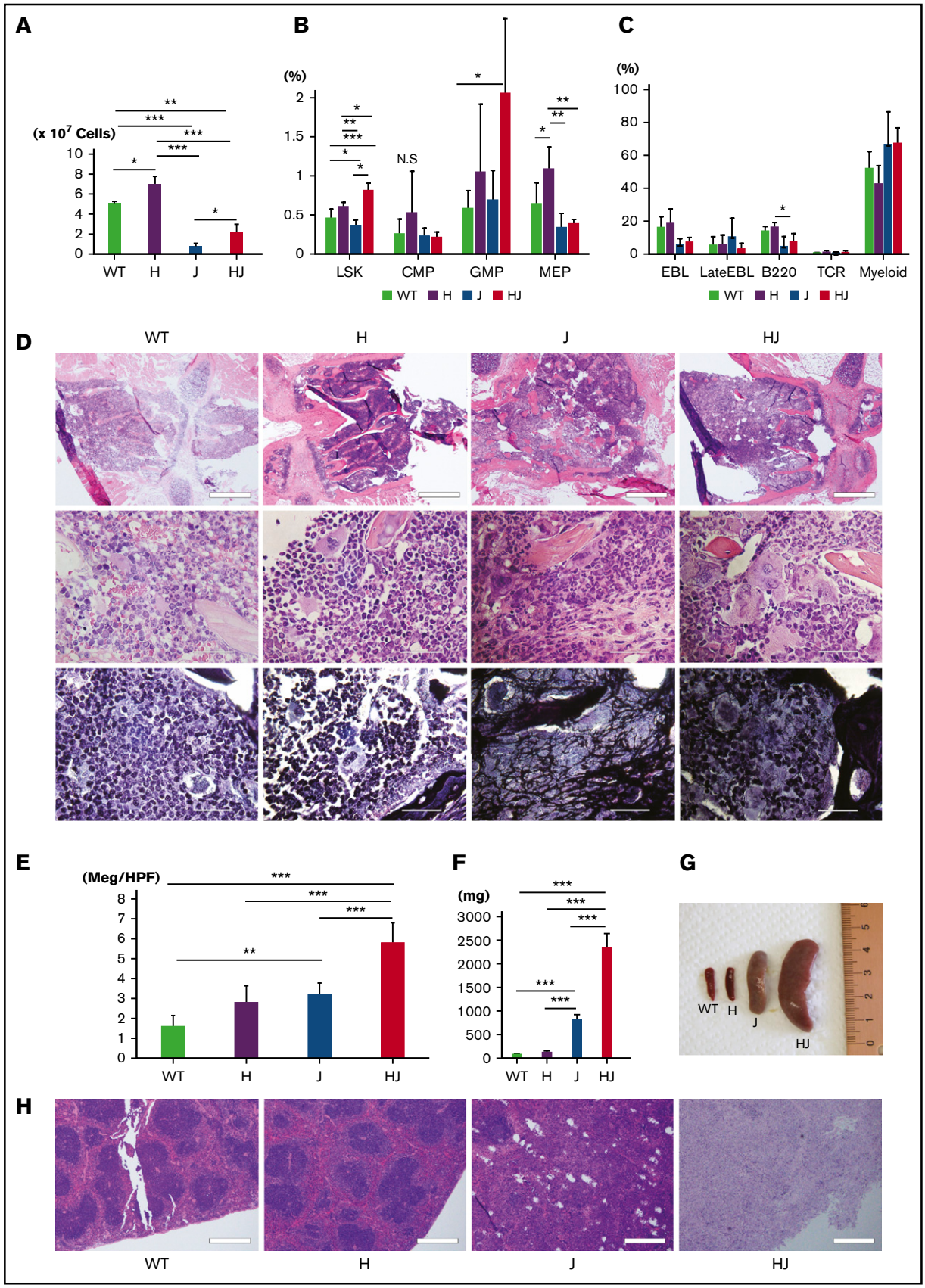
A
(x 10^7 Cells)
WT
H
J
HJ
B
(%)
LSK
CMP
GMP
MEP
N.S
WT H J HJ
C
(%)
EBL
LateEBL
B220
TCR
Myeloid
WT H J HJ
D
WT
H
J
HJ
E
(Meg/HPF)
WT
H
J
HJ
F
(mg)
WT H J HJ
G
WT
H
J
HJ
H
WT
H
J
HJ

Figure 2.

HMGA2 expression is negatively regulated by *MIRlet-7* microRNAs,[24] and high *HMGA2* mRNA levels were correlated with reduced *MIRlet-7* in some patients with MPNs.[21] We have generated transgenic (tg) mice harboring *Hmga2* complementary DNA (cDNA) with a truncated 3′ untranslated region (UTR) (Δ*Hmga2*), thereby lacking binding sites of *MIRlet-7* that repress Hmga2 expression.[25] Δ*Hmga2* mice overexpress Hmga2, develop ET-like disease, and their hematopoietic cells exhibit a clonal advantage against wild-type (WT) cells at the hematopoietic stem cell (HSC) level in serial bone marrow (BM) transplants (BMTs). Alternatively, endogenous Hmga2 expression is upregulated by the loss of *Bmi1* or *Ezh2* in conjunction with *Arf/Ink4a*-knockout (KO)[26] or *JAK2*V617F[27-29] in mice representing more severe MF than mice with *Arf/Ink4a*-KO or *JAK2*V617F alone.

HMGA2 is important for the self-renewal of fetal HSCs, but is not expressed in normal adult tissues and hematopoiesis,[30] whereas various cancer cells overexpress *HMGA2*.[31,32] *HMGA2* mRNA is overexpressed in hematopoietic cells of most patients with PMF,[21,22,33] but its direct role in the MPNs remains unknown. Here, because most MPN patients with high *HMGA2* mRNA levels harbor a driver mutation represented by *JAK2*V617F,[21] we studied mice carrying both $JAK2^{V617F}$ and overexpression of Hmga2 due to tg-Δ*Hmga2* ($\Delta Hmga2/JAK2^{V617F}$) or conditional deletion of *Ezh2* ($JAK2^{V617F}/Ezh2^{\Delta}$). The present study revealed that Hmga2 directly promotes progression of MPN with *JAK2*V617F and, correspondingly, severe MPN of $JAK2^{V617F}/Ezh2^{\Delta/WT}$ mice can be rescued by deletion of *Hmga2*; the study also revealed that *MIRlet-7* suppression and polycomb-recessive complex 2 (PRC2) mutations correlated with the elevated *HMGA2* mRNA levels in patients with PMF.

Materials and methods

Mice

All mice were on a C57BL6/J background and analyzed 12 weeks after birth or 8 weeks after BMT unless otherwise specified. Δ*Hmga2* mice[25] and $JAK2^{V617F}$ mice (line 2 with MF generated from BDF-1 by backcrossing with WT C57BL6/J mice)[13,34] were previously described. $Ezh2^{flox/flox}$ mice[35] were crossed with *Rosa26::Cre*-ERT mice (TaconicArtemis GmbH, Köln, Germany), and deletion of *Ezh2* was induced by intraperitoneal administration of 1 mg per day tamoxifen (Sigma-Aldrich, St. Louis, MO) in corn oil (Sigma-Aldrich) for 5 consecutive days from 4 weeks after BMT. $HMGA2^{-/WT}$ mice,[36] and Ly5.2$^+$ and Ly5.1$^+$ WT mice were purchased from The Jackson Laboratory (Bar Harbor, ME), CLEA (Tokyo, Japan), and RIKEN-BRC (Tsukuba, Japan). Peripheral blood cells were counted by XT-1800i (Sysmex, Kobe, Japan). All studies were approved by the Animal Study Committee of Fukushima Medical University.

Histopathology

Hematoxylin-eosin, silver, and anti-HMGA2 stains (Spring Bioscience, Pleasanton, CA) were performed for paraffin-embedded samples with standard protocols. Pictures were taken and digitized by a DP73 microscope with CellSens software (Olympus, Tokyo, Japan).

Cells

From mice, peripheral leukocytes were obtained by lysing samples with Pharm Lyse (BD, Franklin Lakes, NJ). BM nuclear cells were collected by grinding bones, and mononuclear cells (MNCs) were separated by centrifugation through Ficoll Histopaque (Sigma-Aldrich). The patients' granulocytes were separated by centrifugation through Ficoll Lymphosepar I (IBL, Gunma, Japan).[21]

Flow cytometry

Flow cytometry was performed using a FACSCanto II (BD). Cells were stained with fluorescein isothiocyanate (FITC)-Ter119, phycoerythrin (PE)-CD71, eFluora 450–B220, peridinin chlorophyll (PerCP)/Cy5.5–T-cell receptor β (TCRβ), and allophycocyanin (APC)-Gr1; or PerCP/Cy5.5-Sca-I, PE/Cy7-cKit, Alexa647-CD34, PE-CD16/32, FITC-CD41, and Biotin-Lineage (CD3e, CD4, CD5, CD8a, CD11, B220, Ter119, and Gr1) followed by visualization with APC/Cy7-streptavidin. For chimerism analyses, eFluora450-B220, PerCP/Cy5.5-TCRβ, APC-CD45.1, and PE-CD45.2 (all from eBioscience, San Diego, CA) were used. Phosflow with phosphorylated STAT3 (pSTAT3) antibody (BD) was performed according to the manufacturers' protocol.

Colony assay

On a 35-mm plate, BM MNCs were cultured in 1 mL of semisolid methylcellulose medium. For colony-forming unit–erythroid (CFU-E), 1×10^5 cells were cultured in M3234 (StemCell Technologies, Vancouver, BC, Canada) with or without human erythropoietin (EPO; Bioworld Technology, St. Louis Park, MN), and the colony numbers were counted after 3 days. For myeloid colonies, 1×10^4 cells were cultured in M3434 (StemCell Technologies) and colonies were counted after 5 days.

Western blotting

The total protein was extracted from 1×10^7 BM MNCs using CelLytic M buffer (Sigma-Aldrich) containing a protease inhibitor cocktail (Sigma-Aldrich). The samples were subjected to sodium dodecyl sulfate polyacrylamide gel electrophoresis, transferred to a

Figure 2. Hmga2 expression augments BM cells and HSCs with enhancing extramedullary hematopoiesis in $JAK2^{V617F}$-induced MPN. (A) The total nuclear cell numbers from the ground right femur ($\times 10^7$). N = 3 for each. (B) The ratio of each fraction in BM by fluorescence-activated cell sorter (FACS; percentage in all gated cells) is shown. N = 5 for WT, 5 H, 4 J, and 3 HJ mice. (C) Ratios of differentiated cells in BM (percentage in all gated cells). N = 3 for each genotype. (D) Sternal BM histology. Hematoxylin and eosin (top and middle) and silver (bottom) stains. Scale bars indicate 500 μm (top; original magnification ×40) and 50 μm (middle and bottom; original magnification ×1000). (E) Mean megakaryocyte counts in high-powered field (Meg/HPF; ×400). Mean of 5 fields are shown in each genotype. (F) Spleen weight (N = 4, each genotype). (G) Representative picture of the spleens from the littermates. (H) Histology of spleens (hematoxylin and eosin stain). Scale bars indicate 500 μm (original magnification ×40). (A-C, E-F) Bars show the means ± SEM. *$P < .05$; **$P < .01$; ***$P < .001$ (Tukey-HSD test). B220, B220$^+$ B cell; CMP, common myeloid progenitor cell; EBL, CD71$^+$Ter119$^+$ erythroblast; GMP, granulocyte-macrophage progenitor cell; H, Δ*Hmga2*; HJ, $\Delta Hmga2/JAK2^{V617F}$; J, $JAK2^{V617F}$; LateEBL/Ret, CD71$^+$Ter119^{dim} late erythroblast/reticulocyte; MEP, megakaryocyte-erythroid progenitor cell; Myeloid, Gr-1$^+$ myeloid cell; N.S., not significant; T, TCR$^+$ T cell.

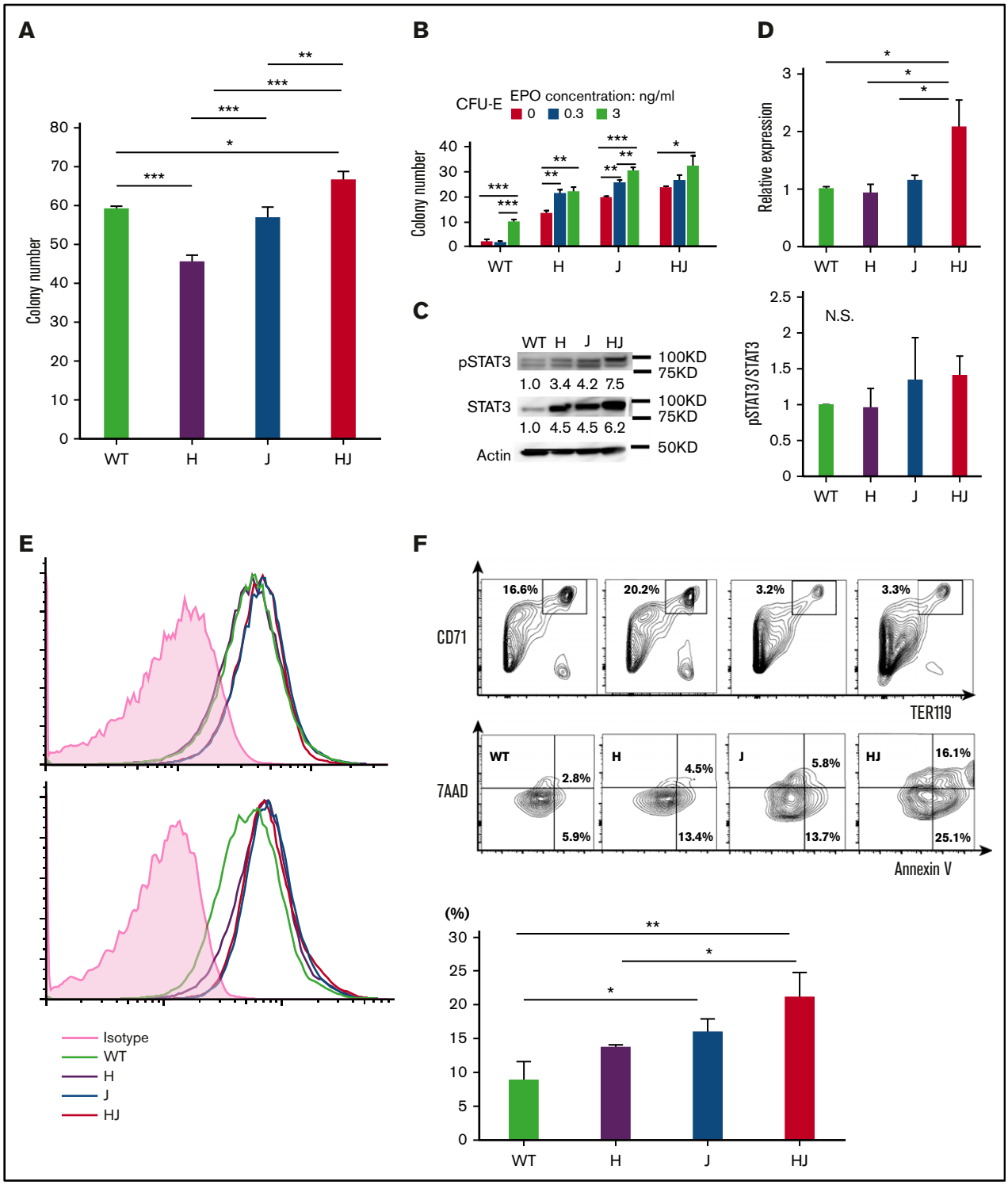

Figure 3. Stat3 activation and apoptotic erythroblasts in Δ*Hmga2*/*JAK2*^{V617F} mice. (A) Myeloid colonies from 1 × 10^4 BM MNCs (N = 3 for each genotype, means ± SEM). *$P < .05$; **$P < .01$; ***$P < .001$ (Tukey-HSD tests). (B) Numbers of CFU-E colonies (means ± SEM) from 1 × 10^5 of BM MNCs (N = 3 for each genotype). *$P < .05$; **$P < .01$; ***$P < .001$ (Tukey-HSD tests). The *P* values calculated by ANOVA were <.01 for both EPO concentrations and mouse transgenes. (C) Western blotting of Stat3 and pStat3 in BM MNCs without cytokine stimulation in each tg mouse. Left panel, A representative result; right panel, mean pSTAT3/STAT3 concentration (from 2 independent experiments) relative to WT. (D) *Stat3* mRNA in BM MNCs by qRT-PCR (means ± SEM; N = 3 for each). *$P < .05$ (Tukey-HSD test). (E) FACS for pStat3 in BM MNCs incubated in the absence (top) and presence (bottom) of IL-3. The horizontal and vertical axes, respectively, indicate the brightness of pStat3 and the cell counts. (F) FACS for apoptosis of $CD71^+Ter119^+$ erythroblasts by Annexin V/7-Aminoactinomycin D (7AAD) staining. Top panel, A representative result; bottom panel, mean ratio of Annexin $V^+/7AAD^-$ apoptotic erythroblasts from 3 independent experiments. *$P < .05$; **$P < .01$; ***$P < .001$ (Tukey-HSD tests). (A-F) H, Δ*Hmga2*; J, *JAK2*^{V617F}; HJ, Δ*Hmga2*/*JAK2*^{V617F}.

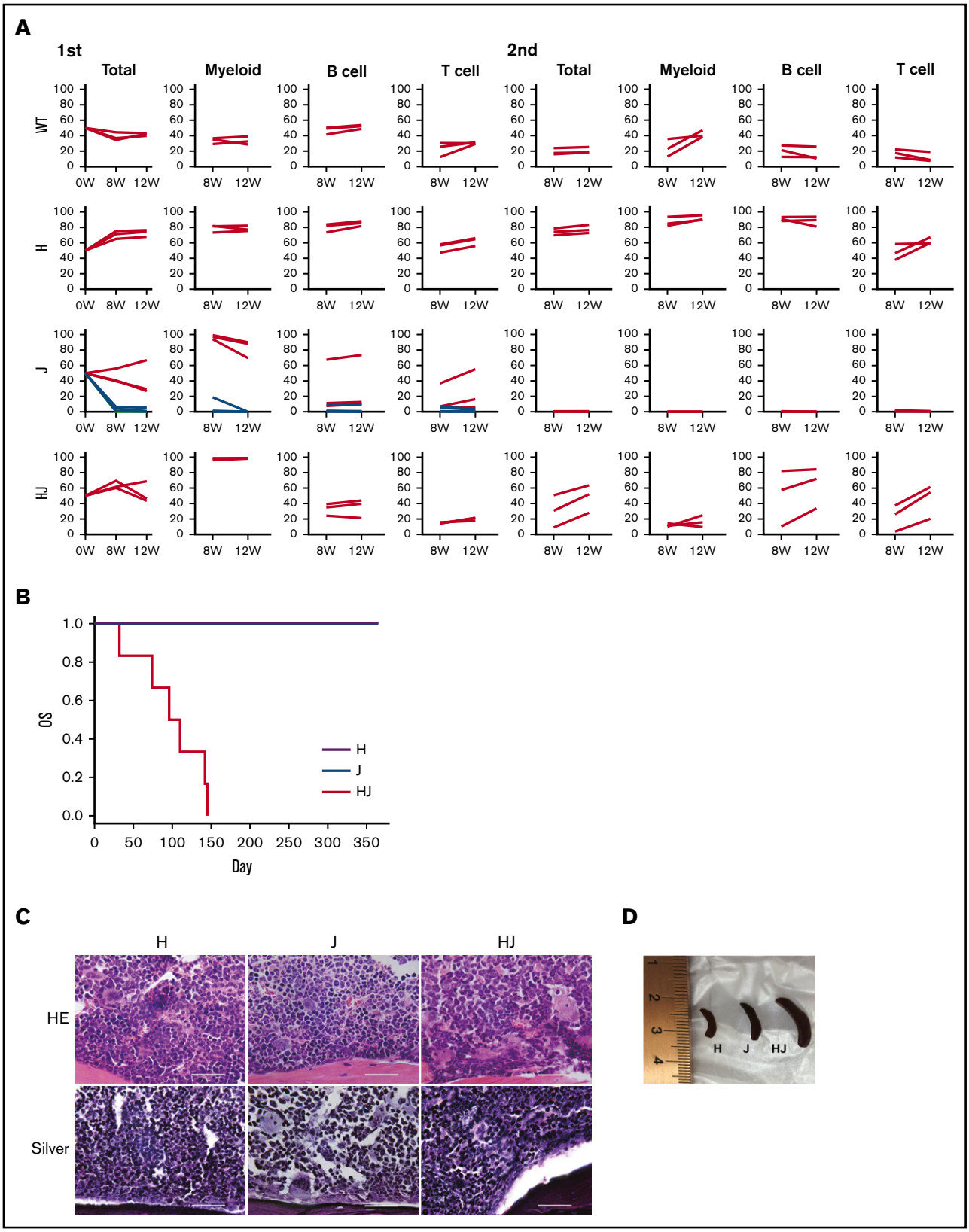

Figure 4. Hmga2 expression promotes the repopulating ability and phenotypic reconstitution of *JAK2*^{V617F}-induced MPN. (A) Competitive repopulations (N = 3-7). Ly5.2^{+} H, J, or HJ BM cells with competitor Ly5.1^{+} WT BM cells at the ratio of 1:1 were injected into lethally irradiated Ly5.1^{+} mice. The ratios (percentage; vertical axis) of Ly5.2^{+} cells in lineages at the indicated time points (horizontal axis) after the first (left) and second (right) BMT are shown. BM cells collected 12 weeks after first BMT were injected

nitrocellulose membrane (GE Healthcare Life Sciences, Uppsala, Sweden), blocked with 5% bovine serum albumin (Wako, Tokyo, Japan), and probed with primary antibodies to Stat3, pStat3 (Cell Signaling Technology, Beverly, MA), actin, and anti-rabbit or anti-mouse horseradish peroxidase (HRP)-conjugated secondary antibody (Santa Cruz Biotechnology, Dallas, TX). The signals were detected with the LAS3000 (Fujitsu, Tokyo, Japan), and densities of bands were measured using ImageJ (version 1.50i; NIH, Bethesda, MD).

BMT

Recipient mice were lethally irradiated (9.0 Gy) 24 hours before BMT and cells were injected IV under anesthesia with isoflurane (Intervet, Osaka, Japan). In the competitive repopulations, 2.5×10^6 Ly5.2$^+$ BM cells with the same number of Ly5.1$^+$ WT BM cells were injected into Ly5.1$^+$ mice. Serial BMTs were performed from these recipients to other lethally irradiated Ly5.1$^+$ mice. For phenotypic reconstitution, 5.0×10^6 BM cells were injected.

RNA sequencing

Each preparation of RNA extracted from flow-sorted BM lineage$^-$ Sca1$^+$cKit$^+$ cells (LSKs) and CD71$^+$Ter119$^+$ erythroblasts using an RNeasy Mini kit (Qiagen, Hilden, Germany) was subjected to reverse transcription (RT) and amplification for 14 cycles, respectively, with the SMARTer Ultra Low Input RNA kit for Sequencing v3 (Clontech, Palo Alto, CA). The double strand–cDNA was fragmented using the S220 Focused ultrasonicator (Covaris), then cDNA libraries were generated using a NEBNext Ultra DNA Library Prep kit (New England BioLabs, Beverly, MA). Sequencing was performed using HiSeq1500 (Illumina) with a single-read sequencing length of 60 bp. After mapping the reference genes to mm10 with TopHat v2.0.13, fragments per kilobase of exon per million reads mapped (FPKM) and reads per kilobase of exon per million reads mapped (RPKM) values were calculated using Cufflinks v2.2.1. After omitting the genes with $<$0.3 FPKM/RPKM values, values were used for evaluation of gene expressions and detections of affected gene sets by gene set enrichment analysis (GSEA; Broad Institute, Cambridge, MA). Genes with $>$1.5-fold upregulation were also applied to the pathway analysis using Ingenuity Pathways Analysis (IPA; Qiagen). Principal component analysis and statistical significance for overlapping genes among genotypes were evaluated according to the RPKM values with 0.5 of the pseudo count using R 3.3.0 (R Foundation, Vienna, Austria). Gene sets with both $<$.05 nominal P values and $<$0.25 false discovery rate (FDR) q values were determined as significantly affected sets in GSEA. Pathways with a z score $>$ |2| were considered to be significant for IPA.

Patients

We studied 45 patients (27 ET, 18 PMF), including 15 patients who were enrolled in our previous study.[21] The diagnosis was made according to World Health Organization (WHO) 2008 criteria,[37] and peripheral blood samples were collected at the time of examination. Samples from 13 healthy volunteers served as controls. The present study was approved by the Ethics Review Board of Fukushima Medical University, which is guided by local policy, national law, and the Declaration of Helsinki. Written informed consent was obtained from each patient and healthy volunteer.

qRT-PCR

The total RNA extracted from granulocytes was used for RT with RevarTra Ace qPCR RT Master Mix (TOYOBO, Osaka, Japan) and the TaqMan MicroRNA RT kit (LifeTechnologies, Carlsbad, CA) for mRNA and microRNA, respectively. Quantitative RT–polymerase chain reaction (qRT-PCR) was performed using a TP800 (Takara, Otsu, Japan) followed by data analysis with Multiplate RQ software (Takara) using the comparative cycle threshold method. RNA levels were determined as relative to *HPRT1* and *U6* noncoding RNA for mRNA and microRNA, respectively. The upper limit of the *HMGA2* mRNA level in granulocytes (1.0) was determined in our former study according to +2 standard deviations (SDs) of the mean value in 13 healthy volunteers.[21] The lower limit level of *MIRlet-7c* in granulocytes was determined according to −2SD of the mean value of 15 healthy volunteers. The primers and probes are listed in supplemental Table 1.

Mutation analysis

Genomic DNA was extracted from the patients' peripheral leukocytes using the QIAamp DNA Mini kit (Qiagen) for screening of mutations in *JAK2*, *MPL*,and *CALR*[38-40] and the target sequence for 50 genes[41] in a GeneRead DNAseq panel for human myeloid neoplasms (Qiagen) using a MiSeq (Illumina). The data were analyzed by the Qiagen NGS Data Analysis web portal. Silent mutations and known germ line polymorphisms in the National Center for Biotechnology Information single nucleotide polymorphism public database were excluded.

Statistics

Statistical significance was determined by an unpaired 2-tailed Student t test, the Tukey–honest significant difference (HSD) test, or 2-way factorial analysis of variance. Survival differences were measured by a log-rank test. All statistical analyses were performed using R3.3.0.

Results

Hmga2 promotes progression of MPN in *JAK2*^{V617F} mice

First, we crossed Δ*Hmga2* mice with *JAK2*V617F-tg (*JAK2*^{V617F}) mice (Figure 1A). WT, Δ*Hmga2*/*JAK2*^{WT} (Δ*Hmga2*), *Hmga2*^{WT}*JAK2*^{V617F} (*JAK2*^{V617F}), and Δ*Hmga2*/*JAK2*^{V617F} mice were born at expected Mendelian ratios. At 12 weeks old, *JAK2*^{V617F} mice showed leukocytosis and anemia; we previously reported the similar trend in mice with *JAK2*V617F of BDF-1[13] and C57BL6/J[27,34] backgrounds. However, leukocytosis and anemia were most severe in Δ*Hmga2*/*JAK2*^{V617F} mice (Figure 1B). Neutrophilia without proliferation of blasts was prominent in Δ*Hmga2*/*JAK2*^{V617F} mice

Figure 4. (continued) for recipients of the secondary BMT. Among J (*JAK2*^{V617F}) mice (N = 7), BM cells from mice that achieved engraftment at the first BMT (red lines, N = 3) were exclusively referred to the second BMT. (B) Kaplan-Meier survival curves, (C) sternal BM histology, and (D) representative picture of the spleens of recipient mice at 12 weeks after the BMT, in BMT from the indicated transgenic mice without competitors (N = 6 for each). (B) P values were calculated by a log-rank test. (C) Hematoxylin-eosin (HE) and silver stains are shown (original magnification ×400). Scale bars indicate 50 μm. H, Δ*Hmga2*; J, *JAK2*^{V617F}; HJ, Δ*Hmga2*/*JAK2*^{V617F}.

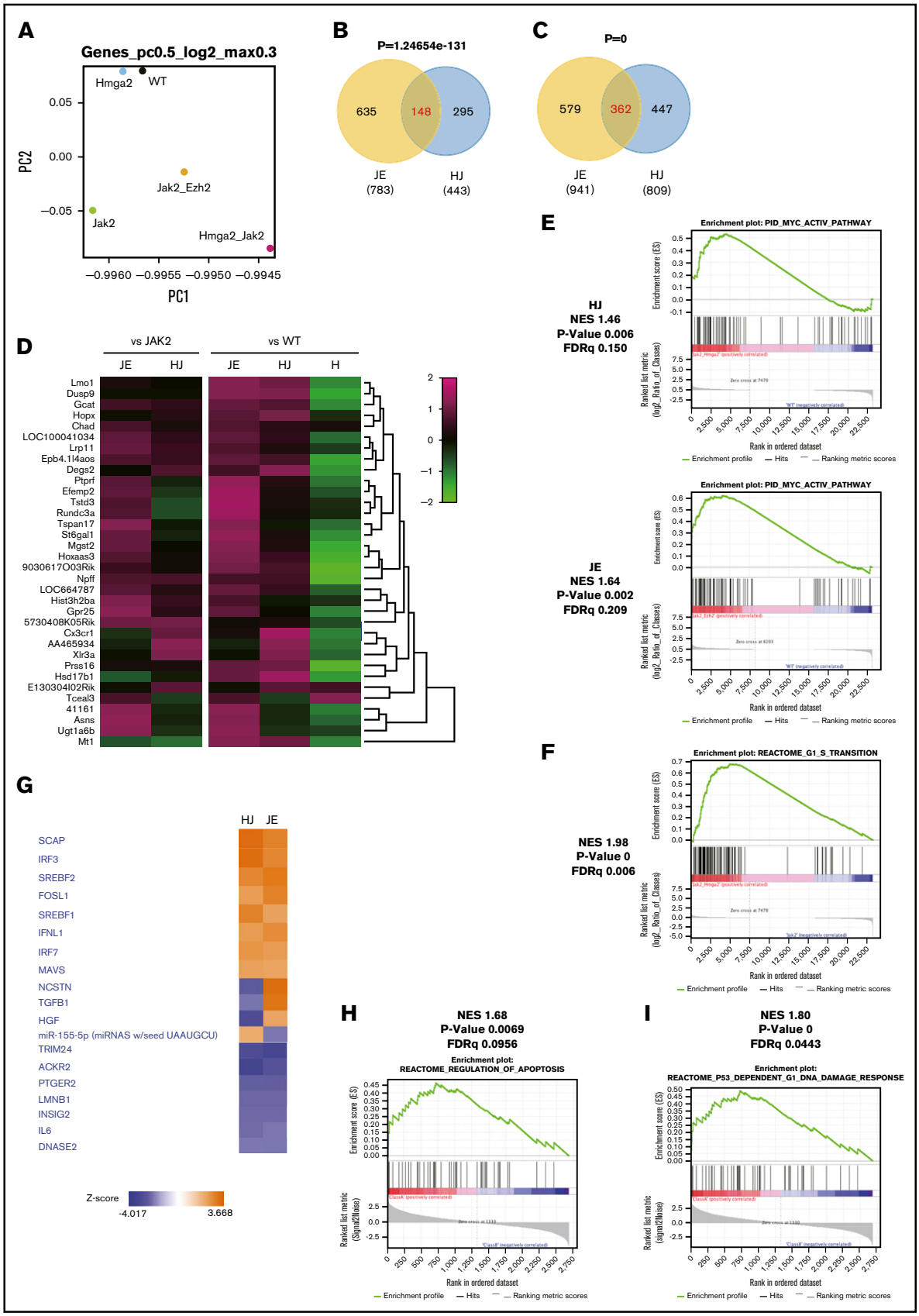
A
Genes_pc0.5_log2_max0.3
Hmga2
WT
Jak2_Ezh2
Jak2
Hmga2_Jak2
PC2
PC1
B
P=1.24654e-131
635
148
295
JE (783)
HJ (443)
C
P=0
579
362
447
JE (941)
HJ (809)
D
vs JAK2
vs WT
JE
HJ
H
E
HJ
NES 1.46
P-Value 0.006
FDRq 0.150
JE
NES 1.64
P-Value 0.002
FDRq 0.209
Enrichment plot: PID_MYC_ACTIV_PATHWAY
Rank in ordered dataset
F
NES 1.98
P-Value 0
FDRq 0.006
Enrichment plot: REACTOME_G1_S_TRANSITION
G
HJ
JE
SCAP
IRF3
SREBF2
FOSL1
SREBF1
IFNL1
IRF7
MAVS
NCSTN
TGFB1
HGF
miR-155-5p (miRNAS w/seed UAAUGCU)
TRIM24
ACKR2
PTGER2
LMNB1
INSIG2
IL6
DNASE2
Z-score
-4.017
3.668
H
NES 1.68
P-Value 0.0069
FDRq 0.0956
Enrichment plot: REACTOME_REGULATION_OF_APOPTOSIS
I
NES 1.80
P-Value 0
FDRq 0.0443
Enrichment plot: REACTOME_P53_DEPENDENT_G1_DNA_DAMAGE_RESPONSE

Figure 5.

(Figure 1C-D). The Δ*Hmga2*/*JAK2*^{V617F} mice died within 150 days, whereas other mice survived for over 1 year (Figure 1E). The number of BM nuclear cells were increased in Δ*Hmga2* mice but decreased in *JAK2*^{V617F} mice, and they were partially restored in Δ*Hmga2*/*JAK2*^{V617F} mice (Figure 2A). In the presence of *JAK2*V617F, Hmga2 augmented the ratio of hematopoietic stem and progenitor cell (HSPC)-enriched LSKs (Figure 2B), but not erythroblasts (Figure 2C). Modest increases of granulocyte-macrophage progenitor and Gr1^{+} cells were observed in the *JAK2*^{V617F} and Δ*Hmga2*/*JAK2*^{V617F} mice (Figure 2B-C). Megakaryocytes were more proliferative in Δ*Hmga2* and *Jak2*^{V617F} mice compared with WT mice, and were further increased in Δ*Hmga2*/*Jak2*^{V617F} mice without morphologic change (Figure 2D-E). *JAK2*^{V617F} and Δ*Hmga2*/*JAK2*^{V617F} BM were equally fibrotic; there was no MF in the WT or Δ*Hmga2* BM (Figure 2D). Splenomegaly was more remarkable and the splenic structures were destroyed in Δ*Hmga2*/*JAK2*^{V617F} mice compared with both Δ*Hmga2* and *JAK2*^{V617F} mice (Figure 2F-H). BM cells showed slight increases in myeloid colonies in Δ*Hmga2*/*JAK2*^{V617F} mice (Figure 3A). All of the Δ*Hmga2*, *JAK2*^{V617F}, and Δ*Hmga2*/*JAK2*^{V617F} BM showed EPO-independent erythroid-colony formation, an important feature of MPN. The colony numbers were the highest in Δ*Hmga2*/*JAK2*^{V617F} for each EPO concentration, and the difference became smaller as the EPO concentration increased (Figure 3B).

We sought the basis of the severe phenotype in Δ*Hmga2*/*JAK2*^{V617F} mice. Based on a recent finding on the importance of STAT3 in MPNs,[42] we investigated the Stat3 status. We found increased expression of *Stat3* mRNA and protein in BM MNCs of Δ*Hmga2*/*JAK2*^{V617F} mice compared with Δ*Hmga2* and *JAK2*^{V617F} mice (Figure 3C-D), whereas the basal Stat3 phosphorylation was comparable among these genotypes (Figure 3C,E). We also evaluated the apoptosis of erythroblasts because Δ*Hmga2*/*JAK2*^{V617F} mice presented with more severe anemia despite EPO-independent erythroid-colony formation and similar MF compared with *JAK2*^{V617F} mice. The ratios of erythroblasts were equally altered in *JAK2*^{V617F} and Δ*Hmga2*/*JAK2*^{V617F} BM, but Δ*Hmga2*/*JAK2*^{V617F} erythroblasts were more apoptotic (Figure 3F).

Hmga2 expands the *JAK2*^{V617F} clone and reproduces the severe MPN after BMT

To investigate repopulating ability, we transplanted Ly5.2^{+} Δ*Hmga2*, *JAK2*^{V617F}, or Δ*Hmga2*/*JAK2*^{V617F} BM cells with Ly5.1^{+} competitor cells into lethally irradiated mice. After the initial BMT, Δ*Hmga2*, and Δ*Hmga2*/*JAK2*^{V617F} cells were engrafted in all recipients, whereas *JAK2*^{V617F} cells were <10% in 4 of 7 recipients (Figure 4A). The proportion of the Ly5.2^{+} donor cells were the highest in recipients of Δ*Hmga2* followed by Δ*Hmga2*/*JAK2*^{V617F} in B cells and total cells, and the opposite was found in myeloid cells. After a second BMT, Δ*Hmga2*/*JAK2*^{V617F} cells were less dominant than Δ*Hmga2* cells but were restored, whereas *JAK2*^{V617F} cells were completely rejected (Figure 4A). Δ*Hmga2* cells fully expanded after a third BMT (not shown), confirming the strong repopulating and self-renewal abilities of HSCs overexpressing Hmga2,[25,30] which likely conferred a clonal dominance to *JAK2*^{V617F} cells. Moreover, the BMT from Δ*Hmga2*/*JAK2*^{V617F} mice to WT mice reproduced splenomegaly and proliferation of megakaryocytes in BM, despite not inducing MF (Figure 4C-D). However, mice transplanted with ΔΔ*Hmga2*/*JAK2*^{V617F} cells survived for a shorter time compared with the recipients from single-tg mice (Figure 4B).

Long-term Hmga2 expression causes anemia without MF

The impact of Hmga2 on MF was not evident in BMT. To clarify whether Hmga2 alone induces fibrosis in the long-term, we studied old Δ*Hmga2* mice (supplemental Figure 1). Eventually, 60-week-old Δ*Hmga2* mice exhibited anemia, but ratios of their erythroid progenitors and erythroblasts were not different from old WT mice. They showed moderate splenomegaly, but never developed MF, as confirmed in a considerable number (N = 26). Moreover, the erythroblasts from old Δ*Hmga2* mice were more apoptotic compared with old WT mice. However, serial BMT revealed that cells from old Δ*Hmga2* mice retain a clonal advantage against young WT cells. Taken together, the long-term expression of Hmga2 induces anemia possibly due to the apoptosis of erythroblasts without MF, whereas their HSCs possess the repopulating ability of young Δ*Hmga2* mice.

Gene expression profile in *JAK2*^{V617F} cells with Hmga2 overexpression

HMGA2 changes chromatin structure and binds to AT-rich DNA sequences via AT-hook domains, leading to the upregulations of targets.[43] To identify HMGA2 targets in the setting of MPNs, we performed RNA sequencing (RNA-seq) of LSKs from WT, Δ*Hmga2*, *JAK2*^{V617F}, and Δ*Hmga2*/*JAK2*^{V617F} mice, as well as *JAK2*^{V617F}/*Ezh2*$^{Δ/Δ}$ mice based on recent reports showing that *Ezh2* KO deteriorates MPNs with upregulating endogenous *Hmga2* expression in HSPCs of mice with *JAK2*V617F.[27-29] Relative to WT, Δ*Hmga2*/*JAK2*^{V617F} mice showed the greatest change in the gene expression profile among genotypes (Figure 5A). We found that 148 of 443 genes (33.4%) or 362 of 809 genes (44.7%) were upregulated in Δ*Hmga2*/*JAK2*^{V617F} mice compared with *JAK2*^{V617F} mice or WT mice, respectively, overlapped with those of *JAK2*^{V617F}/*Ezh2*$^{Δ/Δ}$ mice (Figure 5B-C; supplemental Table 2), and that 35 genes, including known oncogenes targeted by Ezh2, *Lmo1*, *Gcat*, and *Prss16*,[44] were common (Figure 5D). There were some commonly enriched gene sets, including those involved in activation of the MYC pathway between Δ*Hmga2*/*JAK2*^{V617F} and *JAK2*^{V617F}/*Ezh2*$^{Δ/Δ}$ mice (Figure 5E). Δ*Hmga2*/*JAK2*^{V617F} LSKs had frequent upregulation of gene

Figure 5. Hmga2 overexpression alters transcription of genes including the targets of Ezh2. (A) A Principal component (PC) analysis based on total gene expression in LSK cells (LSKs) isolated from WT, H, J, HJ, or JE recipient mice (5 for each and mixed for RNA-seq) 4 weeks after tamoxifen injection. (B) Venn diagrams showing upregulated genes between HJ and JE LSKs relative to J. (C) Venn diagrams showing upregulated genes between HJ and JE LSK cells relative to WT. (D) Heatmaps showing the expression of representative genes upregulated in panels B and C. (E) MYC pathway enriched in HJ (top) and JE (bottom) compared with WT. This pathway was not enriched in J (FDR = 0.389). (F) Enrichment plot of G1-S transition (HJ vs J), which represents frequent upregulations of gene sets associated with cell cycle and metabolism in Δ*Hmga2*/*JAK2*^{V617F} LSKs (shown in supplemental Tables 3 and 4). (G) Signal activation/inactivation in HJ and JE mice relative to J shown by an upstream analysis. Pathways with z score > |2| in both HJ and JE are shown. (H) CD71^{+}Ter119^{+} erythroblasts sorted from BM of 12-week-old WT, H, J, and HJ mice (3 for each) were mixed for RNA-seq. Enrichment of gene sets for regulation of apoptosis (HJ vs J) is shown. (I) GSEA of RNA-seq data for p53-dependent G1 DNA damage response pathway in erythroblasts (HJ vs J). H, Δ*Hmga2*; J, *JAK2*^{V617F}; HJ, Δ*Hmga2*/*JAK2*^{V617F}; JE, *JAK2*^{V617F}/*Ezh2*$^{Δ/Δ}$; NES, normalized enrichment score.

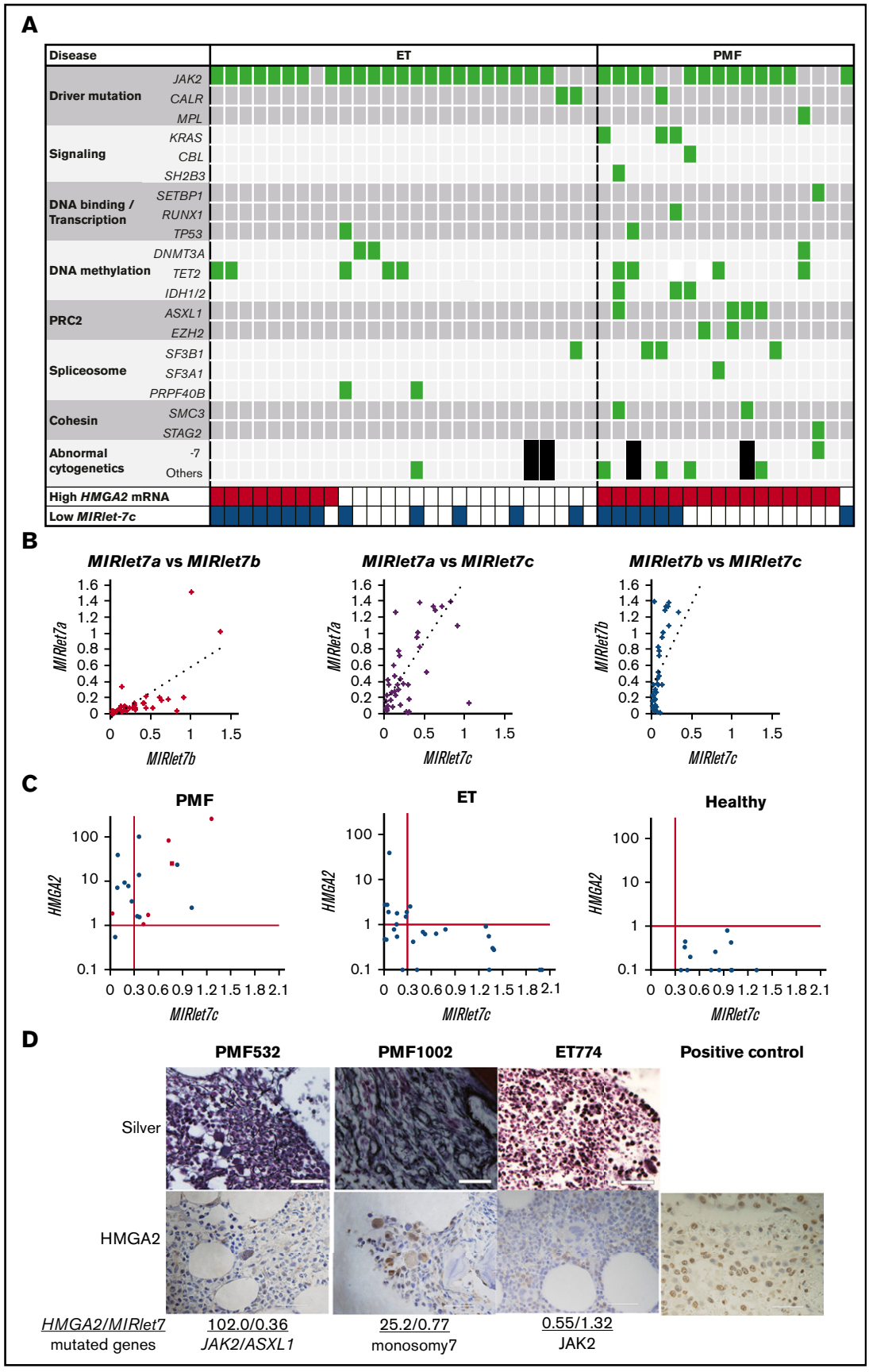
A
Disease
ET
PMF
Driver mutation
JAK2
CALR
MPL
Signaling
KRAS
CBL
SH2B3
DNA binding / Transcription
SETBP1
RUNX1
TP53
DNA methylation
DNMT3A
TET2
IDH1/2
PRC2
ASXL1
EZH2
Spliceosome
SF3B1
SF3A1
PRPF40B
Cohesin
SMC3
STAG2
Abnormal cytogenetics
-7
Others
High HMGA2 mRNA
Low MIRlet-7c
B
MIRlet7a vs MIRlet7b
MIRlet7a vs MIRlet7c
MIRlet7b vs MIRlet7c
MIRlet7a
MIRlet7b
MIRlet7c
C
PMF
ET
Healthy
HMGA2
MIRlet7c
D
PMF532
PMF1002
ET774
Positive control
Silver
HMGA2
HMGA2/MIRlet7
mutated genes
102.0/0.36
JAK2/ASXL1
25.2/0.77
monosomy7
0.55/1.32
JAK2

Figure 6.

sets associated with cell cycle and metabolism (Figure 5F; supplemental Tables 3 and 4). Pathway analysis with IPA also revealed the common activation of several pathways in LSKs of Δ*Hmga2*/*JAK2*^{V617F} and *JAK2*^{V617F}/*Ezh2*$^{Δ/Δ}$ mice compared with those of *JAK2*^{V617F} mice, including chaperone-related *SCAP* and *SREBF1/2* pathways, whereas *TGFB* was upregulated only in those of *JAK2*^{V617F}/*Ezh2*$^{Δ/Δ}$ mice (Figure 5G).

We also investigated CD71^{+}Ter119^{+} erythroblasts by RNA-seq to identify the mechanisms of severe anemia in Δ*Hmga2*/*JAK2*^{V617F} mice. Significantly affected groups (supplemental Tables 5 and 6) included gene sets of apoptosis regulation (Figure 5H) and p53 activation (Figure 5I), which is well known to induce anemia due to apoptosis of erythroid progenitors.[45-47] Moreover, enriched gene sets in erythroblasts were different from those in LSKs. For example, interferon-related genes, involving the JAK-STAT pathway, were enriched in erythroblasts (FDR q = 0.02; supplemental Table 5), but not in LSKs (FDR q > 0.5), of Δ*Hmga2*/*JAK2*^{V617F} mice.

Most patients with PMF highly express *HMGA2* mRNA with the repression of *MIRlet-7* or mutations in PRC2 components

Subsequently, we studied the *HMGA2* mRNA and *MIRlet-7* levels, and mutations in the epigenetic modifiers in patients with MPNs. We focused on ET and PMF because the megakaryocyte lineage is dominant in those groups and an *Ezh2* deletion in megakaryocytes played an important role in the progression of *JAK2*^{V617F}-induced MF.[27] High *HMGA2* mRNA levels were observed in granulocytes of some ET (9 of 27, 33.3%) and most PMF (17 of 18, 94.4%). Most patients had a driver mutation in *JAK2*, *CALR*, or *MPL* in both ET (25 of 27, 92.6%) and PMF (15 of 18, 83.3%). For other investigated genes, most patients with PMF harbored at least 1 additional mutation, whereas ET rarely had such a mutation, except for DNA methylation–related enzymes (Figure 6A; supplemental Table 7). Patients with PMF also carried chromosomal abnormalities; none of them showed 12q rearrangement involving the *HMGA2* locus, whereas 1 patient had monosomy 7, which causes *EZH2* loss.[19]

The expression levels of *MIRlet-7a*, *-7b*, and *-7c* were correlated with each other (Figure 6B), and the expression of *MIRlet-7c* represents those of *MIRlet-7* family members. Interestingly, the reduced *MIRlet-7c* levels were correlated with high *HMGA2* mRNA levels in most patients with ET, but in less than half of the PMF. Patients with MPNs who highly expressed *HMGA2* mRNA (6 of 26, 23.1%) more often harbored monosomy 7 or mutations in PRC2 members, *EZH2* and *ASXL1*, compared with patients without high *HMGA2* expression (0 per 19, 0%; $P = .032$), especially in patients without a reduction in *MIRlet-7* expression (5 of 11, 45.5%) (Figure 6A,C). In contrast, there were no differences in the frequencies of mutations in other gene groups. Therefore, the loss of PRC2 members might be associated with the upregulation of *HMGA2* in patients as in mice.[27-29] We then investigated the expression of HMGA2 in biopsied BM. HMGA2 is highly expressed primarily in hematopoietic cells, especially the nucleus of megakaryocytes (Figure 6D), suggesting the possibility that HMGA2 correlates with proliferation of megakaryocytes in these patients as in *JAK2*^{V617F} mice overexpressing HMGA2.

Depletion of endogenous Hmga2 ameliorates MPN with anemia in *JAK2*^{V617F} mice with the loss of *Ezh2*

To confirm the importance of Hmga2 in MPNs with *JAK2*V617F and the loss of Ezh2, we crossed *Hmga2*-KO (*Hmga2*$^{-/WT}$) mice[36] with *JAK2*^{V617F}/*Ezh2*$^{Δ/Δ}$ mice, and obtained *JAK2*^{V617F}/*Ezh2*$^{Δ/WT}$/*Hmga2*$^{-/WT}$ and *JAK2*^{V617F}/*Ezh2*$^{Δ/WT}$/*Hmga2*$^{WT/WT}$ mice after the second generation. Mice transplanted with *JAK2*^{V617F}/*Ezh2*$^{Δ/Δ}$ cells and those with *JAK2*^{V617F}/*Ezh2*$^{Δ/WT}$ cells showed a similar MPN-like phenotype with more severe anemia, leukocytosis, and splenomegaly compared with mice transplanted with *JAK2*^{V617F} cells,[27] and mimic patients with *EZH2* mutations because mutations in *EZH2* rarely acquire homozygosity in patients.[28] Thus, we performed BMT from *JAK2*^{V617F}/*Ezh2*$^{Δ/WT}$/*Hmga2*$^{-/WT}$ and *JAK2*^{V617F}/*Ezh2*$^{Δ/WT}$/*Hmga2*$^{WT/WT}$ mice (Figure 7A). Strikingly, *JAK2*^{V617F}/*Ezh2*$^{Δ/WT}$/*Hmga2*$^{-/WT}$ recipients, whose *Hmga2* mRNA was suppressed to the basal level (0.9-fold) of *JAK2*^{V617F} mice, revealed significantly reduced splenomegaly, leukocytosis, thrombocythemia, and anemia, compared with *JAK2*^{V617F}/*Ezh2*$^{Δ/+}$/*Hmga2*$^{WT/WT}$ recipients with a twofold higher expression of *Hmga2* mRNA compared with *JAK2*^{V617F} mice (Figure 7B-C).

Discussion

HMGA2 is overexpressed in solid cancers, and is associated with their poor prognosis,[32] but little is known about its role in hematologic diseases. In Δ*Hmga2* mice, Hmga2 is overexpressed by deleting its 3′UTR containing *MIRlet-7*–binding sites; such deletions have been found in a variety of cancers,[24] but are rare in MPNs.[21,33] The truncated *HMGA2* make fusion genes, which may affect the disease phenotype, although *MIRlet-7* is more important for regulation of gene expression than the fusions in vitro.[24] In our former study, none of the 38 patients with high *HMGA2* mRNA levels carried a rearrangement of the *HMGA2* locus, and *MIRlet-7* was low in the majority, but not in all of them.[21] The present study revealed that about half of PMF patients with high *HMGA2* mRNA levels, without the repression of *MIRlet-7*, harbor mutations of PRC2-related *EZH2* and *ASXL1* (Figure 6C). This might be in line with a previous report describing upregulation of *Hmga2* by loss of PRC2 through H3K27 trimethylation.[27] Here, our murine data may imply that Hmga2 is a key player in the progression of MPNs with loss of PRC2 or *MIRlet-7*. First, the addition of 3′UTR-deleted *Hmga2* to

Figure 6. High *HMGA2* mRNA levels in patients with PMF are correlated with either repressed *MIRlet-7* expressions or mutations in PRC2 components. (A) Mutations in the patients with ET (N = 27) and PMF (N = 18). Black squares indicate no metaphase cells in the chromosomal analysis. (B) Correlations in the expression of *MIRlet-7a*, *-7b*, and *-7c* in granulocytes of the patients with ET and PMF. *MIRlet-7a* vs *-7b*, $R = 0.70$ (left); *MIRlet-7a* vs *-7c*, $R = 0.74$ (center); *MIRlet-7b* vs *-7c*, $R = 0.85$ (right) (*R* indicates correlation coefficients). (C) Correlations in the expression levels of *MIRlet-7c* and *HMGA2* mRNA in the granulocytes of individual patients. The red lines indicate the lower (*MIRlet-7c*) or upper (*HMGA2*) limit of the normal range determined according to the data of the healthy controls (see "Materials and methods"). Red circles indicate the patients with mutations in PRC2-related *EZH2* and *ASXL1*, and a rhomboid denotes a patient with monosomy 7 involving *EZH2*. (D) Immunostaining of biopsied BM. The nuclei of megakaryocytes from 2 PMF patients with high expression of *HMGA2* were positively stained by anti-HMGA2 antibody; those of the ET patient with low expression of *HMGA2* were not stained. The tissue from breast cancer, in which the nuclei of neoplastic cells were positively stained, was used as a positive control. Scale bars indicate 50 μm.

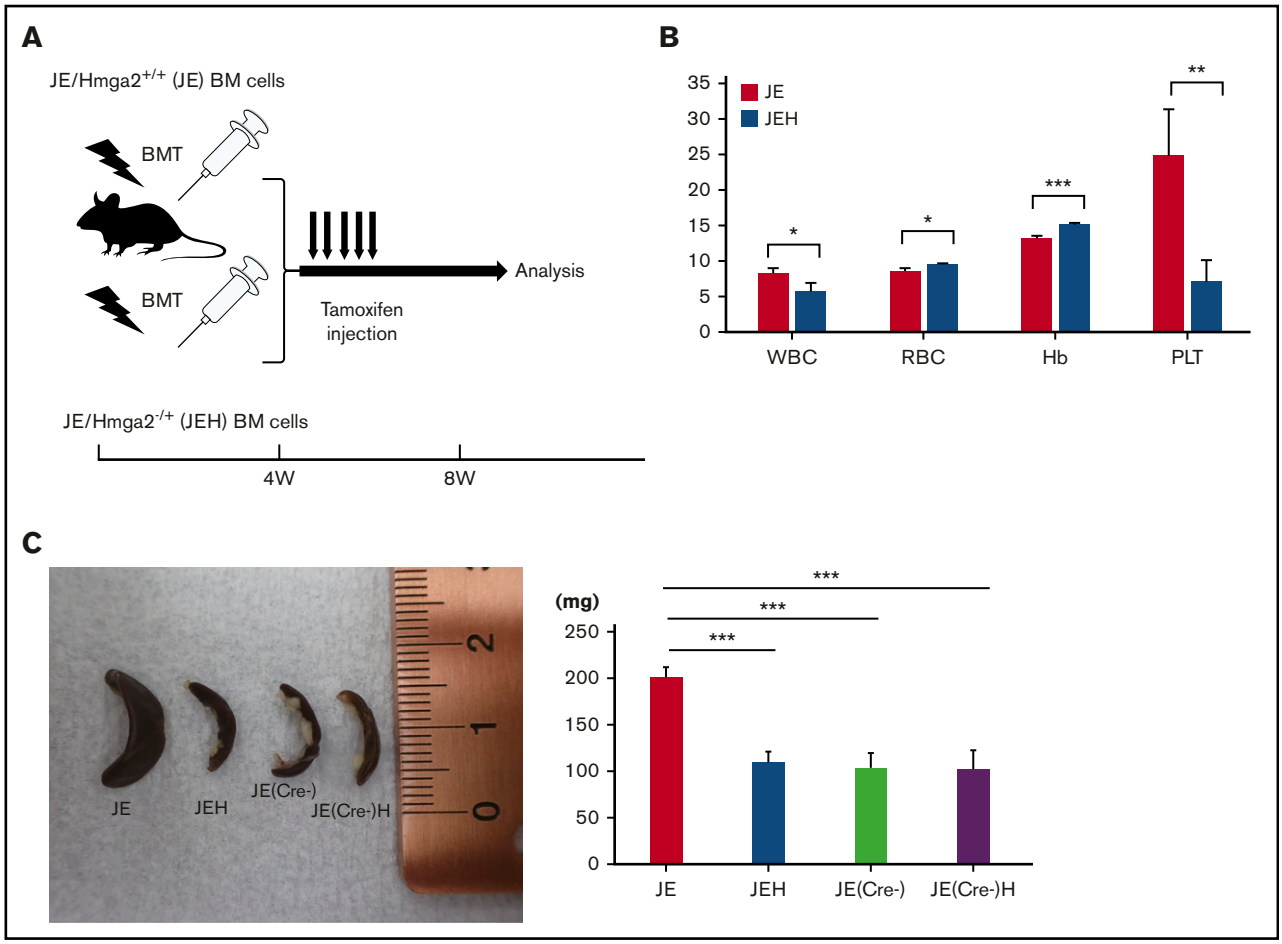

Figure 7. Hmga2 inhibition ameliorates MPN in *JAK2*^{V617F} mice with *Ezh2* KO. (A) Schematic diagram of *Hmga2* KO (*Hmga2*$^{-/+}$) in *JAK2*^{V617F}/*EZH2*$^{flox/WT}$/*CRE*-ERT (JE). BM cells were collected from JE with *HMGA2*$^{-/+}$ (JEH) or *HMGA2*$^{+/+}$ (JE) mice and transplanted. Conditional *Ezh2* KO was initiated by tamoxifen 4 weeks after transplantation. (B) Complete blood cell counts (means ± SEM). N = 5 for each. *$P < .05$; **$P < .01$; ***$P < .001$ (Student *t* test). (C) Spleens at 8 weeks after transplantation with JE, JEH, JE without Cre [JE(Cre−)], and JEH without Cre [JE(Cre−)H] cells. Left, Representative figure. Right, Mean spleen weight. N = 3 for each; ***$P < .001$ (Turkey-HSD test).

JAK2^{V617F} (Δ*Hmga2*/*JAK2*^{V617F}) mice, which represents the disruption of the *MIRlet-7*/*HMGA2* axis in patients with MPNs, markedly exacerbated anemia, leukocytosis, and splenomegaly. These were similarly seen in *JAK2*^{V617F}/*Ezh2*$^{Δ/Δ}$ mice that represent loss of PRC2.[27] Correspondingly, anemia, leukocytosis, and splenomegaly were effectively ameliorated by KO of *Hmga2* in *JAK2*^{V617F}/*Ezh2*$^{Δ/WT}$ mice. Moreover, LSKs of Δ*Hmga2*/*JAK2*^{V617F} mice showed overlapping gene upregulations with *JAK2*^{V617F}/*Ezh2*$^{Δ/Δ}$ mice.

Importantly, cells from Δ*Hmga2*/*JAK2*^{V617F} mice could reconstitute the disease phenotype following the second BMT. The influence of *JAK2*V617F on HSC ability is controversial; some researchers reported that *JAK2*V617F attenuates HSC ability,[9,10,34,48] whereas others showed that *JAK2*V617F increases LSKs and repopulating ability.[11,49] Such differences may come from variations in the strategies of introduction and the expression level of *JAK2*V617F.[48] However, Hmga2 expression conferred a further proliferative capacity to already proliferative *JAK2*^{V617F} cells and improved dominance in serial BMT, although we used the tg-*JAK2*V617F system in which HSC ability may be more impaired than in other systems.[50] Furthermore, LSKs were decreased in *JAK2*^{V617F} BM compared with WT or Δ*Hmga2* BM, and Hmga2 expression restored LSKs to *JAK2*^{V617F} BM (Figure 2B). Thus, Hmga2 may contribute to both proliferation and expansion of an MPN clone at the HSC level, and compensate number and/or function of HSCs impaired by *JAK2*^{V617F}. We also found that BMT recipients from HJ mice showed a similarly shortened survival period (97 days of median survival after the BMT; Figure 4D) as individual tg HJ mice (92 days after the birth, Figure 1E), suggesting that their cause of death was associated with hematologic abnormality. In the recipients of HJ BM, splenomegaly was more severe than in recipients of J BM, while less severe compared with individual HJ mice. On the other hand, moribund recipients of HJ BM consistently showed severe anemia (<5 g/dL hemoglobin) as seen in individual HJ mice, implying that anemia may be a possible cause of death.

In BM MNCs of Δ*Hmga2*/*JAK2*^{V617F} mice, Stat3 expression was higher than in other strains, and some genes involved in the JAK-STAT pathway were upregulated in erythroblasts but not LSKs of Δ*Hmga2*/*JAK2*^{V617F} mice, indicating that differentiated cells are more responsible to proliferative phenotype than HSPC level.

Despite more severe anemia, the severity of MF was similar and BM cell number was not decreased in Δ*Hmga2*/*JAK2*^{V617F} mice compared with *JAK2*^{V617F} mice. Considering that the apoptosis of erythroblasts was increased in Δ*Hmga2*/*JAK2*^{V617F} mice with enrichment of p53 activation (Figure 5H), ineffective erythropoiesis associated with p53-mediated apoptosis[45-47] might be a factor that increases anemia. In contrast to Δ*Hmga2*/*JAK2*^{V617F}, *JAK2*^{V617F}/*Ezh2*$^{Δ/Δ}$ mice presented more severe MF with decreased BM cellularity, compared with *JAK2*^{V617F} mice.[27] In the RNA-seq of LSKs, the transforming growth factor (TGF)–related pathway was upregulated in *JAK2*^{V617F}/*Ezh2*$^{Δ/Δ}$ rather than Δ*Hmga2*/*JAK2*^{V617F} mice, relative to *JAK2*^{V617F} mice. Notably, *TGFBR1* is a direct target of EZH2,[29] and activated TGFB signaling is important to evoke MF.[51-53] Therefore, targets of Ezh2 other than Hmga2 may play a greater role in fibrosis in this context. RNA-seq also revealed that an *Ezh2* deletion and overexpression of *Hmga2* share deregulated oncogenic targets such as *Lmo1*[54-56] in the presence of *JAK2*V617F. These observations give rise to the hypothesis that when the loss of *Ezh2* and/or *MIRlet*-7 block the inhibition of some oncogenes, *Hmga2* may synergistically accelerate such upregulation in the MPN stem cells. Moreover, chaperone-related pathways were affected in both *JAK2*^{V617F}/*Ezh2*$^{Δ/Δ}$ and Δ*Hmga2*/*JAK2*^{V617F} mice (Figure 5E). This may be consistent with the finding that HMGA2 recruits chaperones to alter chromatin structures that contribute to the oncogenic activity of HMGA2.[43,57]

Apart from PMF, our patients with ET did not have a mutation in *EZH2* or *ASXL1*, in agreement with a previous report,[58] and the expression levels of *HMGA2* were inversely correlated with those of *MIRlet*-7 (Figure 6C). Thus, the cause of high expression of *HMGA*2 in these patients may be repression of *MIRlet*-7, but it is unclear how *MIRlet*-7 is downregulated. Lin28b is a well-known negative regulator of *MIRlet*-7.[59,60] Although the *Lin28b*/*MIRlet*-7/*Hmga2* axis regulates the self-renewal of fetal HSCs, *Lin28b* is silenced after birth.[30,61] In agreement, most of our patients did not express *LIN28b* at detectable levels (data not shown). At present, low-level *LIN28B* or other alterations, for example, DNA methylation,[62,63] and NF45/90[64] may be candidates for future investigation.

In conclusion, our study suggests a crucial role of Hmga2 in the progression of MPNs. Amelioration of the severe phenotype in *JAK2*^{V617F} mice with *Ezh2* KO, by inhibition of Hmga2, indicates that *HMGA2* may be one of the most important targets upregulated by mutations of PRC2 components and encourages the development of HMGA2-targeted therapy for patients with high-risk MPNs.

Acknowledgments

The authors thank Toshio Kitamura (The Institute of Medical Science, The University of Tokyo) for PLAT-E cells, Haruhiko Koseki (RIKEN Center for Integrative Medical Sciences) for *Ezh2*$^{Δ/Δ}$ mice, and Minae Takasaki, Ayumi Haneda, Fumiko Miura, and Moe Muramatsu for technical assistance.

This work was supported by grants from the Ministry of Education, Culture, Sports, Science and Technology (26860720 and 16K19582 [K.U.], 24591405 and 15K09484 [K.I.], 15K09457 [K.H.-S.], 15K09483 [K.O.], and 25461920 [T.M.]), and Aplastic Anemia & MDS International Foundation (3048-42179) (K.I.).

Authorship

Contribution: K.U. designed the research, performed experiments, analyzed data, and wrote the manuscript; K.I. designed and supervised the research, performed experiments, analyzed data, and wrote the manuscript; T.I., K.O., Y.S., P.J.M., and M.B. supervised the study; K.H.-S. performed experiments and analyzed data; Y.H. performed histologic study; T.S., H.O., S. Kimura, and A.S.-N. collected and preserved patients' samples and analyzed data; Y.N. performed experiments; T.M. analyzed data; S.M. and N.K. examined mutations; K. Shide and K. Shimoda provided mice and interpreted results; S. Koide, K.A., and M.O. performed RNA-seq; A.I. performed RNA-seq and supervised the study; and Y.T. supervised the study and approved the manuscript.

Conflict-of-interest disclosure: The authors declare no competing financial interests.

Correspondence: Kazuhiko Ikeda, Department of Hematology, Fukushima Medical University, 1 Hikarigaoka, Fukushima 960-1295, Japan; e-mail: kazu-ike@fmu.ac.jp.

References

1. Tefferi A. Pathogenesis of myelofibrosis with myeloid metaplasia. *J Clin Oncol*. 2005;23(33):8520-8530.
2. Levine RL, Gilliland DG. Myeloproliferative disorders. *Blood*. 2008;112(6):2190-2198.
3. Tam CS, Nussenzveig RM, Popat U, et al. The natural history and treatment outcome of blast phase BCR-ABL- myeloproliferative neoplasms. *Blood*. 2008;112(5):1628-1637.
4. Kralovics R, Passamonti F, Buser AS, et al. A gain-of-function mutation of JAK2 in myeloproliferative disorders. *N Engl J Med*. 2005;352(17):1779-1790.
5. James C, Ugo V, Le Couédic JP, et al. A unique clonal JAK2 mutation leading to constitutive signalling causes polycythaemia vera. *Nature*. 2005; 434(7037):1144-1148.
6. Klampfl T, Gisslinger H, Harutyunyan AS, et al. Somatic mutations of calreticulin in myeloproliferative neoplasms. *N Engl J Med*. 2013;369(25): 2379-2390.
7. Nangalia J, Massie CE, Baxter EJ, et al. Somatic CALR mutations in myeloproliferative neoplasms with nonmutated JAK2. *N Engl J Med*. 2013;369(25): 2391-2405.
8. Pardanani AD, Levine RL, Lasho T, et al. MPL515 mutations in myeloproliferative and other myeloid disorders: a study of 1182 patients. *Blood*. 2006; 108(10):3472-3476.
9. Mullally A, Lane SW, Ball B, et al. Physiological Jak2V617F expression causes a lethal myeloproliferative neoplasm with differential effects on hematopoietic stem and progenitor cells. *Cancer Cell*. 2010;17(6):584-596.
10. Li J, Spensberger D, Ahn JS, et al. JAK2 V617F impairs hematopoietic stem cell function in a conditional knock-in mouse model of JAK2 V617F-positive essential thrombocythemia. *Blood*. 2010;116(9):1528-1538.

11. Akada H, Yan D, Zou H, Fiering S, Hutchison RE, Mohi MG. Conditional expression of heterozygous or homozygous Jak2V617F from its endogenous promoter induces a polycythemia vera-like disease. *Blood*. 2010;115(17):3589-3597.

12. Marty C, Lacout C, Martin A, et al. Myeloproliferative neoplasm induced by constitutive expression of JAK2V617F in knock-in mice. *Blood*. 2010;116(5):783-787.

13. Shide K, Shimoda HK, Kumano T, et al. Development of ET, primary myelofibrosis and PV in mice expressing JAK2 V617F. *Leukemia*. 2008;22(1):87-95.

14. Tiedt R, Hao-Shen H, Sobas MA, et al. Ratio of mutant JAK2-V617F to wild-type Jak2 determines the MPD phenotypes in transgenic mice. *Blood*. 2008;111(8):3931-3940.

15. Delhommeau F, Dupont S, Della Valle V, et al. Mutation in TET2 in myeloid cancers. *N Engl J Med*. 2009;360(22):2289-2301.

16. Stegelmann F, Bullinger L, Schlenk RF, et al. DNMT3A mutations in myeloproliferative neoplasms. *Leukemia*. 2011;25(7):1217-1219.

17. Abdel-Wahab O, Pardanani A, Rampal R, Lasho TL, Levine RL, Tefferi A. DNMT3A mutational analysis in primary myelofibrosis, chronic myelomonocytic leukemia and advanced phases of myeloproliferative neoplasms. *Leukemia*. 2011;25(7):1219-1220.

18. Carbuccia N, Murati A, Trouplin V, et al. Mutations of ASXL1 gene in myeloproliferative neoplasms. *Leukemia*. 2009;23(11):2183-2186.

19. Ernst T, Chase AJ, Score J, et al. Inactivating mutations of the histone methyltransferase gene EZH2 in myeloid disorders. *Nat Genet*. 2010;42(8):722-726.

20. Zhan H, Cardozo C, Raza A. MicroRNAs in myeloproliferative neoplasms. *Br J Haematol*. 2013;161(4):471-483.

21. Harada-Shirado K, Ikeda K, Ogawa K, et al. Dysregulation of the MIRLET7/HMGA2 axis with methylation of the CDKN2A promoter in myeloproliferative neoplasms. *Br J Haematol*. 2015;168(3):338-349.

22. Guglielmelli P, Zini R, Bogani C, et al. Molecular profiling of CD34+ cells in idiopathic myelofibrosis identifies a set of disease-associated genes and reveals the clinical significance of Wilms' tumor gene 1 (WT1). *Stem Cells*. 2007;25(1):165-173.

23. Tefferi A, Guglielmelli P, Larson DR, et al. Long-term survival and blast transformation in molecularly annotated essential thrombocythemia, polycythemia vera, and myelofibrosis. *Blood*. 2014;124(16):2507-2513.

24. Mayr C, Hemann MT, Bartel DP. Disrupting the pairing between let-7 and Hmga2 enhances oncogenic transformation. *Science*. 2007;315(5818):1576-1579.

25. Ikeda K, Mason PJ, Bessler M. 3'UTR-truncated Hmga2 cDNA causes MPN-like hematopoiesis by conferring a clonal growth advantage at the level of HSC in mice. *Blood*. 2011;117(22):5860-5869.

26. Oguro H, Yuan J, Tanaka S, et al. Lethal myelofibrosis induced by Bmi1-deficient hematopoietic cells unveils a tumor suppressor function of the polycomb group genes. *J Exp Med*. 2012;209(3):445-454.

27. Sashida G, Wang C, Tomioka T, et al. The loss of Ezh2 drives the pathogenesis of myelofibrosis and sensitizes tumor-initiating cells to bromodomain inhibition. *J Exp Med*. 2016;213(8):1459-1477.

28. Shimizu T, Kubovcakova L, Nienhold R, et al. Loss of Ezh2 synergizes with JAK2-V617F in initiating myeloproliferative neoplasms and promoting myelofibrosis. *J Exp Med*. 2016;213(8):1479-1496.

29. Yang Y, Akada H, Nath D, Hutchison RE, Mohi G. Loss of Ezh2 cooperates with Jak2V617F in the development of myelofibrosis in a mouse model of myeloproliferative neoplasm. *Blood*. 2016;127(26):3410-3423.

30. Copley MR, Babovic S, Benz C, et al. The Lin28b-let-7-Hmga2 axis determines the higher self-renewal potential of fetal haematopoietic stem cells. *Nat Cell Biol*. 2013;15(8):916-925.

31. Fusco A, Fedele M. Roles of HMGA proteins in cancer. *Nat Rev Cancer*. 2007;7(12):899-910.

32. Pallante P, Sepe R, Puca F, Fusco A. High mobility group a proteins as tumor markers. *Front Med (Lausanne)*. 2015;2:15.

33. Andrieux J, Demory JL, Dupriez B, et al. Dysregulation and overexpression of HMGA2 in myelofibrosis with myeloid metaplasia. *Genes Chromosomes Cancer*. 2004;39(1):82-87.

34. Kameda T, Shide K, Yamaji T, et al. Loss of TET2 has dual roles in murine myeloproliferative neoplasms: disease sustainer and disease accelerator. *Blood*. 2015;125(2):304-315.

35. Hirabayashi Y, Suzki N, Tsuboi M, et al. Polycomb limits the neurogenic competence of neural precursor cells to promote astrogenic fate transition. *Neuron*. 2009;63(5):600-613.

36. Zhou X, Benson KF, Ashar HR, Chada K. Mutation responsible for the mouse pygmy phenotype in the developmentally regulated factor HMGI-C. *Nature*. 1995;376(6543):771-774.

37. Vardiman JW, Thiele J, Arber DA, et al. The 2008 revision of the World Health Organization (WHO) classification of myeloid neoplasms and acute leukemia: rationale and important changes. *Blood*. 2009;114(5):937-951.

38. Edahiro Y, Morishita S, Takahashi K, et al. JAK2V617F mutation status and allele burden in classical Ph-negative myeloproliferative neoplasms in Japan. *Int J Hematol*. 2014;99(5):625-634.

39. Takei H, Morishita S, Araki M, et al. Detection of MPLW515L/K mutations and determination of allele frequencies with a single-tube PCR assay [published correction appears in *PLoS One*. 2015;10(4):e0124208]. *PLoS One*. 2014;9(8):e104958.

40. Shirane S, Araki M, Morishita S, et al. JAK2, CALR, and MPL mutation spectrum in Japanese patients with myeloproliferative neoplasms. *Haematologica*. 2015;100(2):e46-e48.

41. Cao M, Shikama Y, Kimura H, et al. Mechanisms of impaired neutrophil migration by microRNAs in myelodysplastic syndromes. *J Immunol*. 2017;198(5):1887-1899.

42. Kleppe M, Kwak M, Koppikar P, et al. JAK-STAT pathway activation in malignant and nonmalignant cells contributes to MPN pathogenesis and therapeutic response. *Cancer Discov*. 2015;5(3):316-331.

43. Narita M, Narita M, Krizhanovsky V, et al. A novel role for high-mobility group a proteins in cellular senescence and heterochromatin formation. *Cell*. 2006; 126(3):503-514.

44. Muto T, Sashida G, Oshima M, et al. Concurrent loss of Ezh2 and Tet2 cooperates in the pathogenesis of myelodysplastic disorders. *J Exp Med*. 2013; 210(12):2627-2639.

45. McGowan KA, Li JZ, Park CY, et al. Ribosomal mutations cause p53-mediated dark skin and pleiotropic effects. *Nat Genet*. 2008;40(8):963-970.

46. Dutt S, Narla A, Lin K, et al. Haploinsufficiency for ribosomal protein genes causes selective activation of p53 in human erythroid progenitor cells. *Blood*. 2011;117(9):2567-2576.

47. Kamio T, Gu BW, Olson TS, Zhang Y, Mason PJ, Bessler M. Mice with a mutation in the Mdm2 gene that interferes with MDM2/ribosomal protein binding develop a defect in erythropoiesis. *PLoS One*. 2016;11(4):e0152263.

48. Lundberg P, Takizawa H, Kubovcakova L, et al. Myeloproliferative neoplasms can be initiated from a single hematopoietic stem cell expressing JAK2-V617F. *J Exp Med*. 2014;211(11):2213-2230.

49. Hasan S, Lacout C, Marty C, et al. JAK2V617F expression in mice amplifies early hematopoietic cells and gives them a competitive advantage that is hampered by IFNα. *Blood*. 2013;122(8):1464-1477.

50. Skoda RC. JAK2 impairs stem cell function? *Blood*. 2010;116(9):1392-1393.

51. Martyré MC, Romquin N, Le Bousse-Kerdiles MC, et al. Transforming growth factor-beta and megakaryocytes in the pathogenesis of idiopathic myelofibrosis. *Br J Haematol*. 1994;88(1):9-16.

52. Johnston JB, Dalal BI, Israels SJ, et al. Deposition of transforming growth factor-beta in the marrow in myelofibrosis, and the intracellular localization and secretion of TGF-beta by leukemic cells. *Am J Clin Pathol*. 1995;103(5):574-582.

53. Vannucchi AM, Bianchi L, Paoletti F, et al. A pathobiologic pathway linking thrombopoietin, GATA-1, and TGF-beta1 in the development of myelofibrosis. *Blood*. 2005;105(9):3493-3501.

54. Zhang Y, Yang J, Wang J, Guo H, Jing N. LMO1 is a novel oncogene in lung cancer, and its overexpression is a new predictive marker for anti-EGFR therapy. *Med Oncol*. 2014;31(8):99.

55. Liu J, Yan P, Jing N, Yang J. LMO1 is a novel oncogene in colorectal cancer and its overexpression is a new predictive marker for anti-EGFR therapy. *Tumour Biol*. 2014;35(8):8161-8167.

56. Oldridge DA, Wood AC, Weichert-Leahey N, et al. Genetic predisposition to neuroblastoma mediated by a LMO1 super-enhancer polymorphism. *Nature*. 2015;528(7582):418-421.

57. Zhang R, Poustovoitov MV, Ye X, et al. Formation of MacroH2A-containing senescence-associated heterochromatin foci and senescence driven by ASF1a and HIRA. *Dev Cell*. 2005;8(1):19-30.

58. Lundberg P, Karow A, Nienhold R, et al. Clonal evolution and clinical correlates of somatic mutations in myeloproliferative neoplasms. *Blood*. 2014; 123(14):2220-2228.

59. Viswanathan SR, Daley GQ, Gregory RI. Selective blockade of microRNA processing by Lin28. *Science*. 2008;320(5872):97-100.

60. Viswanathan SR, Powers JT, Einhorn W, et al. Lin28 promotes transformation and is associated with advanced human malignancies. *Nat Genet*. 2009; 41(7):843-848.

61. Oshima M, Hasegawa N, Mochizuki-Kashio M, et al. Ezh2 regulates the Lin28/let-7 pathway to restrict activation of fetal gene signature in adult hematopoietic stem cells. *Exp Hematol*. 2016;44(4):282-296.

62. Brueckner B, Stresemann C, Kuner R, et al. The human let-7a-3 locus contains an epigenetically regulated microRNA gene with oncogenic function. *Cancer Res*. 2007;67(4):1419-1423.

63. Lu L, Katsaros D, de la Longrais IA, Sochirca O, Yu H. Hypermethylation of let-7a-3 in epithelial ovarian cancer is associated with low insulin-like growth factor-II expression and favorable prognosis. *Cancer Res*. 2007;67(21):10117-10122.

64. Sakamoto S, Aoki K, Higuchi T, et al. The NF90-NF45 complex functions as a negative regulator in the microRNA processing pathway. *Mol Cell Biol*. 2009;29(13):3754-3769.